International Journal of Engineering

Journal Homepage: www.ije.ir

Influence of Load Eccentricity on Structural Response of Slender Hybrid Self-compacting Concrete Columns with Reactive Powder Concrete Shells under Uniaxial Loading

A. A. Salman Al-Taai*, W. A. Waryosh

Civil Engineering Department, College of Engineering, Mustansiriyah University, Baghdad, Iraq

PAPER INFO

Paper history:
Received 01 July2025
Received in revised form 17 August 2025
Accepted 28 August 2025

Keywords:
Hybrid Self-compacting Concrete
Slender Columns
Uniaxial Loading
Outer Shells
Reactive Powder Concrete

ABSTRACT

In this paper, a comprehensive investigation of the behavior of slender hybrid reinforced concrete columns consisting of self-compacting normal concrete (SC-NC) and reactive powder concrete (SC-RPC) shells with eccentric compression at different eccentricity ratios is presented. Three eccentricities (0.25, 0.65, and 0.9) were used to carry out these tests on six specimens, divided into three groups according to the eccentricity ratio. Each group included one reference specimen with a conventional SC-NC shell and one hybrid specimen with an RPC shell. The results showed that RPC contributed to the axial load capacity, and moment capacities. It is found that axial capacity increased by 57.8%, 21.1%, and 46.9% for small, medium, and large eccentricities, and moment capacity can increase by up to 56%. The RPC-reinforced specimens demonstrated higher absorption energy and lower lateral deflections. The results validate the effectiveness of RPC to improve the structural performance and behavior of hybrid columns subjected to eccentric uniaxial loading and the findings may offer relevant insights for applications in seismic-resistant and high-rise structures.

***doi**: 10.5829/ije.2026.39.08b.18*

Graphical Abstract

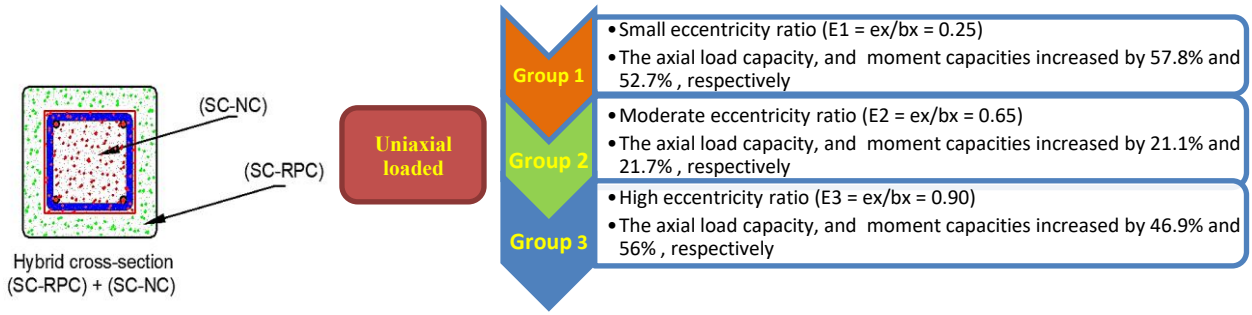

1. INTRODUCTION

RC columns are generally divided into two types in terms of their slenderness, namely slender and short columns, which are widely used in structural design of modern architectural buildings like high-rise buildings, large shopping malls, multilayer car parks, sports stadiums and so on. Being relatively small in transverse sectional dimension and having advantages of design flexibility and space saving, slender RC columns are prone to be more unstable because of the interaction of axial forces and bending moments (1-3). In order to overcome these structural drawbacks, there has been great effort to develop slender hybrid and composite columns by

*Corresponding Author Email: inm.ala@atu.edu.iq
(A. A. Salman Al-Taai)

Please cite this article as: Salman Al-Taai AA, Waryosh WA. Influence of Load Eccentricity on Structural Response of Slender Hybrid Self-compacting Concrete Columns with Reactive Powder Concrete Shells under Uniaxial Loading. International Journal of Engineering, Transactions B: Applications. 2026;39(08):2022-34.

combining different material characteristics for the improvement of the mechanical behaviors and the failure resistance.

A large number of studies have investigated on the structural behavior of composite column systems, especially those with embedded I-section steel profiles in concrete matrix (4-7). Meanwhile, extensive amount of research attention has also been directed to fill concrete-filled steel tube (CFST) columns, with a steel tube boundary and a concrete core (8-13). Furthermore, the mechanical properties of S-CFATCs have been studied extensively in recent years, Some experimental and analytical studies are introduced (14-19).

Hybrid columns (HC), which consist of ordinary concrete core encased with high strength concrete shell, ara an advanced structural form to improve the axial performance (20, 21). This type of hybrid column is considered an advanced structural configuration as it combines the benefits of high-strength concrete with the practicality and cost-efficiency of normal self-compacting concrete in a composite section, aiming to optimize both performance and material economy. The shell serves a two-fold purpose: structurally it can resist up to 40% of the overall axial load and functionally, it enables environmental protection for the embedded steel reinforcement, reducing the potential for corrosion and thermal stresses. As a result, any type of shell damage (whether in the form of surface cracking or material weakening) may adversely affect the strength and overall behavior of the column system (22).

The mechanical behavior of an outer high-strength concrete shell and an inner core may be developed to be full or partial bond in hybrid columns, and will perform differently. Early research work, for example that of Ali, and Mohammed (23), Ali (24), have scrutinized the effects of partial bonding on the ultimate behavior of short hybrid RC columns.

Ali and Mohammed (23) studied the effect of the RPC shell on axial capacity of hybrid columns under eccentric loading based on changing precast RPC shell with normal-strength concrete cover thickness. The results showed that the capacity of the load was improved by about 11% by increasing the shell thickness from 25 mm to 50 mm. The presence of both longitudinal and transverse steel reinforcement also enhanced the ductility and capacity at failure of the members, relative to the unconfined specimens. Also Ali (24) studied the behavior of hybrid columns as external energy-dissipating and self-centering systems by introducing the application of an epoxy layer for high-strength outer shells connected to the precast core. All of these columns were subjected to axial compression followed by eccentric compression, resulting in significant enhancements in ultimate capacity, varying from 28% up to 80% in concentric loading conditions (depending on the compressive strength of the shell). There were also comparable performance improvements with eccentric loading.

There has been a substantial literature published such as Ali and Mahdi (25), Resheq (20), Hamid et al. (26), Al-Zuhairi et al. (21), Mohammed et al. (27) and Mufja (28), studying the structural behavior of hybrid reinforced concrete columns with good bond quality between the high strength outer shell and the normal strength concrete core. The enhancement in axial capacity is attributed to the high strength of the outer shell, confinement effects, and stress redistribution due to full bonding between the core and outer layers.

Ali and Mahdi (25) also explored the effect of various outer shell concrete types—high strength concrete (HSC) and steel fiber reinforced concrete (SFRC) and e/h ratio on behavior of this type of structures. His conclusions were in favor of better shell quality as a noticeable improvement in strength and efficiency. The HSC-wrapped specimens showed a strength increase of 3.74% and 21.08% at eccentricity ratios of 1/3 and 1/2, respectively, whereas SFRC strengthened columns showed strength enhancement of 3.74% and 11.11%, respectively. Resheq (20) studied the axial behavior of hybrid concrete column subjected to axial loading by taking the diameter ratio of the concrete columns (NC) and (SCC) components. Results showed that the decrease of the NC core diameter along with the enlargement of the SCC shell can improve axial load capacity by about 70%. On the other hand, an increase in the NC shell with a decrease in the SCC core resulted in only ∼20% enhancement. Al-Zuhairi et al. (21) analyzed the structural performance of varying hybrid ratios in short columns under biaxial loading. Their study also found that hybrid CFT columns displayed a 33.5% increase in ultimate capacity compared to their nonhybrid counterparts. Moreover, the load-bearing capacity was increased by 38% at 0.16 hybrid ratio after the hybrid ratio was decreased from 0.36 to 0.16, and estimated axial strain also decreased significantly in the similar loading conditions. Hamid et al. (26) investigated the effects of core and transverse reinforcement diameters in short hybrid columns, which consist of ordinary concrete core located between 40 mm RPC layer. This combination enhanced the axial load capacity of the concrete specimens by an impressive 179 per cent compared to standard concrete blocks. Their results also showed that transverse reinforcement had a greater impact on structural strengthening than longitudinal reinforcement.

Previous studies have demonstrated that the mechanical response of hybrid columns with outer high-strength shells varies significantly depending on bonding conditions and shell configuration. These investigations primarily focused on enhancing axial capacity through shell thickness, reinforcement detailing, or interface

treatment, yet further exploration is still needed to evaluate composite performance under eccentric loading in vertically cast systems.

Recent studies have further confirmed that the structural performance of hybrid concrete columns is significantly influenced by the shell type, hybrid ratio, and reinforcement configuration. Improvements in axial strength across various configurations highlight the importance of shell-core interaction, yet comprehensive evaluations under biaxial or eccentric conditions remain limited.

Two commonly practiced methods of producing hybrid columns are widely referred to the literature. The first utilizes a core of plain or low-strength concrete concentrically surrounded by a layer of high-strength, fiber or non-fiber reinforced concrete. This results in a two-concrete cross section optimized for better structural effectiveness.

The hybridized sectioned variables also depend drastically on the rheology of both the concretes. They must, in fact, have been sufficiently fluid and cohesive to permit the outer shell to be cast effectively and remain continuously bonded. Shortcomings in these requirements may lead to chemical homogeneity loss and then structural integrity damage (29-31). Therefore, the use of SCC for the core and the shell could result in better homogeneity and interface compatibility. However, the axial deformation behavior of SCC-contained hybrid columns is not well addressed in the literature to date. A thorough experimental research is necessary to investigate the performance of such systems in axial loading, especially when both concretes meet the requirements of the SCC.

Although empirical work covering the biaxial behavior of long hybrid columns made with self-compacting concrete has been searched for, at the time of this writing there is no literature on their performance. This represents a substantial lack of knowledge of uniaxially loaded hybrid systems behavior, in particular when a complete bond between core and shell is supposed.

Thus, The aim of this study is to experimentally assess the structural performance of slender hybrid columns under eccentric loading, focusing on full-bond interlocking behavior. Recent investigations have highlighted the strategic role of advanced hybrid systems in enhancing structural resilience and controlling dynamic responses, particularly in seismic-prone and tall structures, motivating further exploration into their flexural and energy dissipation behavior (32, 33).

2. TEST SPECIMEN

The models used in this investigation were long RC columns of 140 × 140 mm cross-section and a total height of 1260 mm. Four 10 mm diameter longitudinal steel bars were placed throughout the length of each column, resulting in a reinforcement ratio (ρ) of 1.6%. The 22.5 mm thick on the concrete covers. This detailing adhered to the minimum reinforcement regulations specified in ACI 318-19 (1). The steel bars employed had a yield strength of 630 MPa and a modulus of elasticity of 200 GPa. Close links of 6 mm diameter were provided at 140 mm spacing over height of each column. A plan of the specimen with its dimensions and the reinforcement detailing is presented in Figure 1.

Uniaxial eccentric loading was applied by attaching a pair of corbels to the end of each column, as depicted in Figure 1. These corbels were arranged to carry the full load of the columns and to ensure that the failure takes place in the mid-span area. Corbel cross section was 260 × 260-mm square and 280-mm deep. In order to accomplish objectives of this study a particular test set-up has been developed to simulate the behavior of long columns under eccentric load. This arrangement was made to have load carried, and failure to occur on, the targeted test zone at the center height of the column. The specimens were positioned near the corbel edge to apply the required eccentricity (e/h). The center of gravity (CG) of each cross-section was calculated, and the load was aligned accordingly to ensure consistent eccentric loading.

3. TEST MATRIX

The test matrix of this study, conducted on six specimens, is given in Table 1 and specimens were bilaterally identical. Key parameters were the type of concrete of the

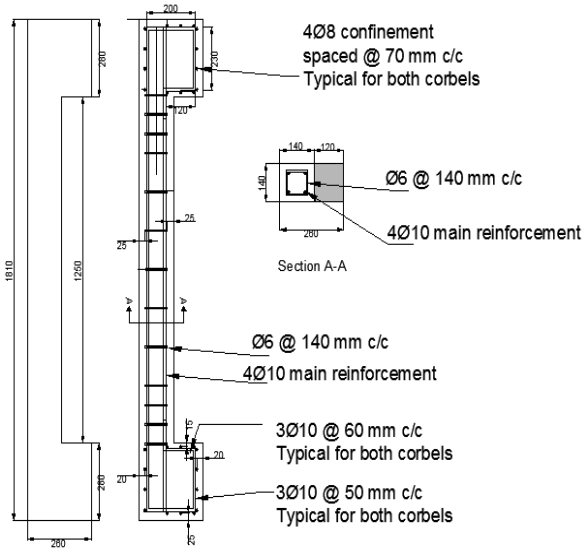

Figure 1. Details of reinforcement for hybrid self-compacting concrete columns

external shell and the degree of loading eccentricity. The specimens subjected to uniaxial eccentric loading were categorized into three groups according to the eccentricity ratio; small, intermediate and large. The types were also named as follows:

- UE1 for a small eccentricity ratio (E1 = ex/bx = 0.25)
- UE2 for a moderate eccentricity ratio (E2 = ex/bx = 0.65)
- UE3 for a high eccentricity ratio (E3 = ex/bx = 0.9)

where, (ex) is the eccentricity in millimeters and (bx) is the width of the column section. The symbol "U" signifies that the specimens were subjected to uniaxial eccentric loading.

Each group consisted of two samples; one reference and one hybrid sample. The control specimens were identified as NUE1, NUE2 and NUE3; and they were produced using self-compacting normal concrete. These served as control specimens. The hybrid elements with the RPC in the shell were denoted as RUE1, RUE2, RUE3, which represent minor, medium, large eccentric distance ratios, respectively. The letters "N" and "R" refer to normal self-compacting concrete and self-compacting reactive powder concrete for the outer section, respectively. Details and the test matrix are given in Table 1.

For future research, it is advisable to explore a larger number of concrete strengths and reinforcement densities, concrete cover sizes and eccentricities in the two principal directions of the section.

4. SPECIMEN INSTRUMENTATION

Specimens were tested under uniaxial eccentric loading in a 3000-kN-capacity testing machine. Loading tests were performed on all columns to failure under increasing load control. An instrumentation configuration per specimen is depicted in Figure 2.

Linear Variable Differential Transformers (LVDTs) were installed to record the lateral displacements, while electrical strain gauges were applied to record the longitudinal strains in the reinforcement located in the mid-height of the columns, as depicted in Figure 2.
The LVDTs were placed on the tension (long) side of the model at three locations: bottom (0), middle (½), and top (full effective length) of the member to record the lateral displacement along the longitudinal direction.

TABLE 1. The test matrix for uniaxial loading

Group	Eccentricity ratio	Self-compacting Hybrid concrete (SC-HC)				
		Outer Shell concrete		Inner Core concrete		designation
		Concrete type	Grade (Mpa)	Concrete type	Grade (Mpa)	Specimens
1	$e_x/b_x = 0.25$ (compression-controlled failure)	SC-NC	33.79	SC-NC	33.79	NUE1
		SC-RPC	88.86			RUE1
2	$e_x/b_x = 0.65$ (tension-controlled failure)	SC-NC	33.79			NUE2
		SC-RPC	88.86			RUE2
3	$e_x/b_x = 0.9$ (tension-controlled failure)	SC-NC	33.79			NUE3
		SC-RPC	88.86			RUE3

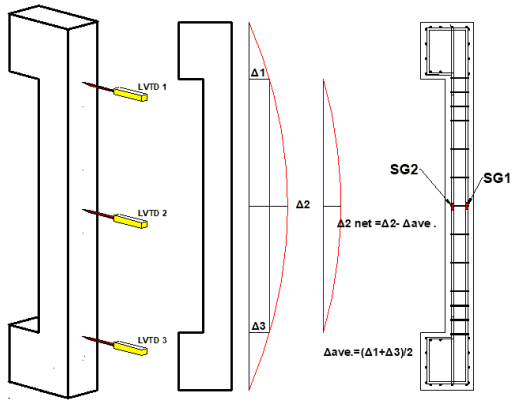

Figure 2. Arrangement of LVDTs and strain gage on longitudinal reinforcement for specimens

At mid-height, gauges SG #1 and SG #2 were pasted to measure strains in the steel bars at the tension and compression sides respectively.

Strain gauges were placed at mid-height where maximum axial strain is typically observed in slender columns. LVDTs were positioned at mid-span to capture the highest lateral deflection, and net readings were calculated by subtracting the middle LVDT value from the average of the other two to eliminate the effect of cross-section rotation and localize measurements between the corbels.

All LVDTs and strain gauges were calibrated according to the manufacturer's procedures prior to testing. The measurement uncertainty was within ±0.05 mm for LVDTs and ±1 με for strain gauges, ensuring

reliable data collection throughout the experiment.

Load was increased to failure in 10 kN increments. All recorded load, strain and displacement data during testing were stored on a computer by data acquisition systems (DAQ) incorporated in the testing machine.

5. TEST SETUP

Figure 3 Test setup for loading to each of the specimens. The load was applied by hydraulic jack through the two-loading caps with semicircular grooves. Hinged connections were used at each end of the columns. Each loading cap was comprised of a top plate (270 × 150 × 40 mm) attached to two side plates (270 × 150 × 10 mm) and two half side plates (150 × 150 × 10 mm). This model was developed in order to prevent stress concentration and early failure in the load path.

Eccentricity was applied and slip was prevented by seating a circular steel rod within semicircular grooves machined in the top loading plate. This configuration acted as a hinge, ensuring stable eccentric loading and allowing rotation. The setup is illustrated in Figure 3. Semicircular cuts were made in the top plates of the caps at defined locations. This resulted in the possibility of controlled uniaxial eccentric loading, depicted in Figure 3. The grooves facilitated the load transmission path only through the plate surfaces of the semicircular grooves, which was useful in the case of equal load transfer during testing.

6. MATERIAL

Multiple trial mixes were adopted to cast an appropriate self-consolidating concrete and the optimum mix design was chosen following EFNARC (33). Two of the original mixes were used in this experiment: Mix 1 is a reference mixture that is typical concrete having a 30 MPa compressive strength and Mix 2 is RPC6380, with 90 MPa in compressive strength.

Figure 3. Test setup and loading condition

The specific ingredients for the two mixes are given in Table 2. Type I ordinary Portland cement in accordance with ASTM type I and Iraqi standard (IQS 5/2019) was used in all mixtures. The coarse aggregate was crushed natural stone with a maximum size of 10 mm and a sulphate content of 0.06%. The fine aggregate used was crushed stone sand (of 3.5 FM) with sulphur content of 0.12 %.Silica fume (SiO_2 content:92%) was adopted as a cementitious replacement material. Straight steel fibers of 13 mm length and 0.2 mm diameter were utilized, which had an aspect ratio (l/df) of 65 and a tensile strength of 2500 MPa.

In order to make it workable and strong enough to be accepted as a self-compacting concrete all mixes were improved with superplasticizer of high efficiency based on modified polycarboxylic ether (Master Glenium 54) furnished by MBCC GROUP. The admixture is brown in colour and the specific gravity is 1.07 and the pH is between 5 and 8 as indicated by technical datasheet. It meets the requirements of ASTM C494 type F and G (34). The dosage was varied to ensure that each mix gave a slump flow of higher than 600 mm, which is the value required forself-compactingconcrete (33).

The 28-day compressive strengths of Mixes 1 and 2 were obtained as 33.79 MPa and 88.86 MPa, respectively. The longitudinal steel was deformed bars (Grade 520) of 10 mm diameter and a yield strength of 630 MPa. Shear reinforcement consisted of 6-mm-dia plain steel bars (i.e. with a yield strength greater than 520 N/mm^2). Mechanical properties of the reinforcement used in the tested specimens are summarized in Table 3.

TABLE 2. Mix proportions of self-compact concrete mixes

Material	Mixes	
	SC-NC	SC-RPC
Cement (Kg/m^3)	360	950
Sand (Kg/m^3)	780	1050
Gravel (Kg/m^3)	830	/
Water (Kg/m^3)	158.5	209.76
Water/Cement ratio	0.44	0.184
MasterGlenium 54 (Kg/m^3)	6.4	45.6
Silica fume (Kg/m^3)	/	190
Silica fume(%)	/	20%
Steel fiber (Kg)	/	78.5
Steel fiber (%)	/	1%
Compressive strength(28-days) (MPa)	33.79	88.86

TABLE 3. Mechanical properties of composite reinforcement

Reinforcement	Yield strength	Ultimate strength
Diameter (6 mm)	526	580
Diameter (8 mm)	354	561
Diameter (10 mm)	630	691

7. CASTING COLUMN SPECIMENS

All column specimens were cast in the vertical direction. For the hybrid reinforced concrete (RC) columns, a square aluminum tube (100 × 100 × 1.5 cm) was installed in the steel mold as a core form. This tube isolated the core concrete from the shell concrete during casting. At its top it was pressed against the steel mold edges to keep it from lateral movement and facilitate its breakaway once cast. The conventional RC columns, on the other hand, were cast at once and have no internal aluminum tube. Complete bonding between the core and the outer shell was ensured by casting both layers simultaneously in a fresh-to-fresh condition. Figure 4 explained cross-section in hybrid self-compacting concrete columns.

8. RESULTS

8. 1. Loads - Lateral Deflection Results From Figures 5 to 7, one can observe the influence of outer shell concrete type of the hybrid columns on the behavior under uniaxial eccentric loading in load-lateral deflection at mid-height. These are the first, second, and third sets of specimens with the eccentricity ratios (e/h = 0.25), (e/h = 0.65), and (e/h = 0.9), respectively. The outer shell material was per each group shifted from self-compacting normal concrete (SC-NC) to self-compacting reactive powder concrete (SC-RPC).

The lateral deflection was measured utilizing three LVDTs (two at the starting and ending point of the test area and one at center height). The net midpoint deflection was accordingly determined.

Experimental results for specimens with uniaxial eccentric loading are summarized in Table 4 and shown in Figure 8. The obtained Pu, Δu, and the percent of change of Pu in comparison to control specimens are displayed in the tabulated form. The findings revealed that the replacement of liner of normal concrete (NC) with reactive powder concrete (RPC) has significantly improved the axial load performance. With the small eccentricity (ex/bx = 0.25), the RUE1 was increased by 57.837% more than that of the control sample (NUE1).For moderate eccentricity (ex/bx = 0.60), RUE2 showed an enhancement of 21.052% relative to NUE2.For a large eccentricity (ex/bx = 0.9), a 46.89% increase in axial capacity compared to the reference sample NUE3 was achieved by RUE3.

Although each group included only two specimens, the percentage variation in peak load values ranged from approximately 19% to 45%, which is within acceptable experimental limits and supports the qualitative reliability of the results.

Although the specimen with e/h = 0.90 (RUE3) experienced the highest eccentricity, its performance in terms of flexural resistance was enhanced by the tensile strength and post-cracking behavior of the RPC shell. The embedded fibers within RPC contributed to stress redistribution by bridging micro-cracks, thereby improving ductility and sustaining load after cracking. In contrast, RUE2 (e/h = 0.65) was also subjected to tensile stresses but to a lesser extent, which may have limited the activation of fiber bridging mechanisms, resulting in earlier failure under a higher peak load (180.94 kN for RUE2 vs. 144.02 kN for RUE3). Meanwhile, RUE1 (e/h = 0.25) failed primarily due to compressive crushing, as the nearly concentric load induced high axial compressive stresses with minimal tension development.

TABLE 4. The experimental findings (ultimate load and displacement) for uniaxially loaded specimens

No.	Specimen	Pu (kn)	Δ_u (mm)	Increase in Pu %
1	NUE1	467.27	7.655	0
2	RUE1	737.52	6.281	57.837
3	NUE2	180.94	20.07	0
4	RUE2	219.04	20.64	21.052
5	NUE3	98.037	17.52	0
6	RUE3	144.02	26.03	46.898

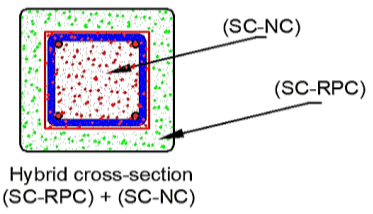

Figure 4. Explained cross-section in hybrid self-compacting concrete columns

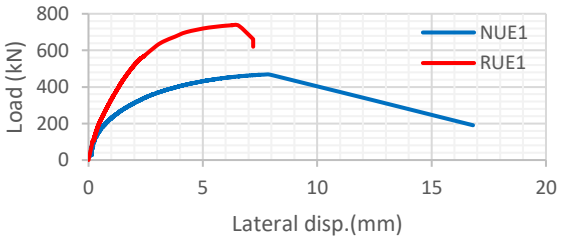

Figure 5. Loads-Lateral deflection curves for low eccentricity ratio (e/h=0.25)

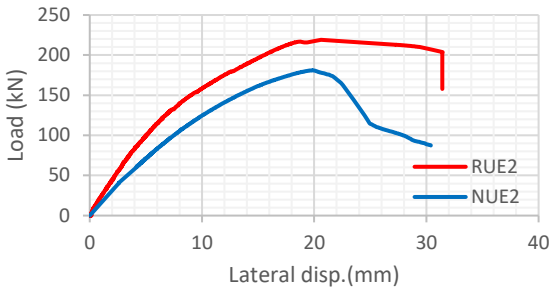

Figure 6. Loads-Lateral deflection curves for medium eccentricity ratio (e/h=0.65)

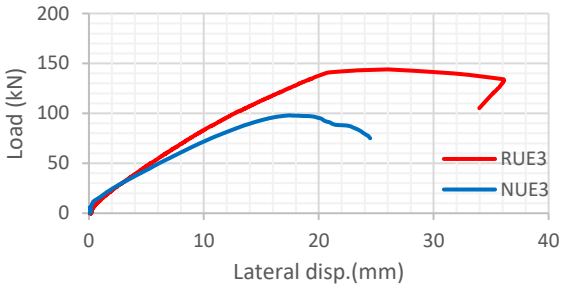

Figure 7. Loads-Lateral deflection curves for large eccentricity ratio (e/h=0.9)

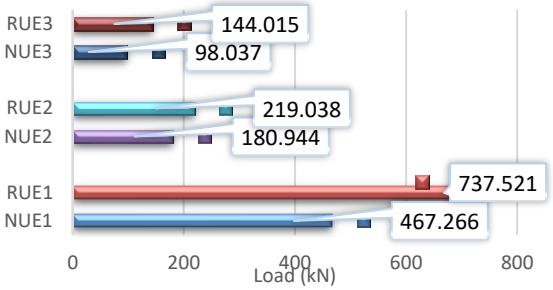

Figure 8. Ultimate load for column's specimens

8. 2. Longitudinal Steel Reinforcement Strains

Figures 9, 10, and 11 show how the longitudinal strain changed on both the compression and tension sides at the mid-height of the specimens in groups one, two, and three, respectively. These figures reveal that, in the uniaxial specimens, the tensile reinforcement reached yield before failure. For small eccentricity (e/h = 0.25), yielding happened at 92% of the ultimate load in specimen NUE1 and 97% in RUE1. This is because the applied eccentricity was small and below the balanced eccentricity of the section. At medium eccentricity (e/h = 0.65), the steel yielded at 87% of the ultimate load in NUE2 and at 88% in RUE2. This was due to increased section rotation, larger deflections, and an eccentricity higher than the balanced value. For large eccentricity (e/h = 0.9), yielding occurred at 81% of the ultimate load in NUE3 and 76% in RUE3. The lower values were caused by even more section rotation and significantly higher deflections, with the eccentricity well above the balanced level.

In all uniaxial specimens it was obvious that the compression reinforced concrete had not yielded. This means that the failure mode was controlled by tension, rather than un-restrained compression.

Thus the failure mode was ductile, and the influence of the level of eccentricity, the same as that for the tension reinforcement, and the position of the tension reinforcement near the outermost tension fiber were significant.

For uniaxially loaded columns, the maximum tensile stress generally occurs on the outer tension surface, leading to failure by yielding of the tensile steel prior to the occurrence of compressive concrete failure.

8. 3. Moment–curvature Relationship

All specimens were loaded under eccentric compression, resulting in uniaxial bending. The moment–curvature relationship was studied in the principal direction of the

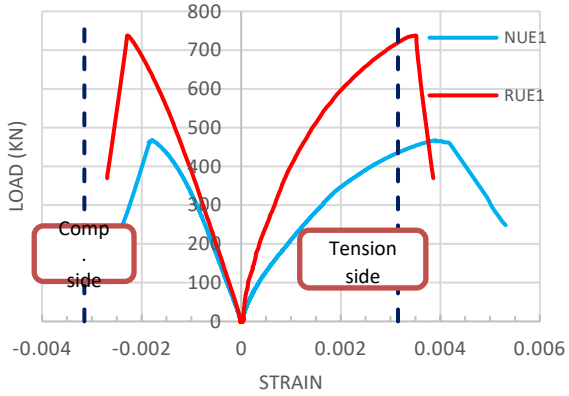

Figure 9. load -longitudinal steel strain curves for medium eccentricity ratio (e/h=0.25)

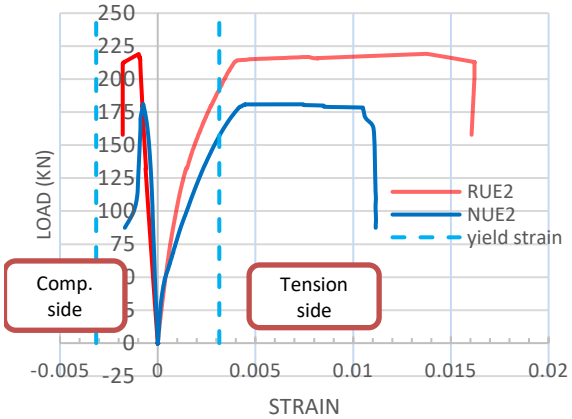

Figure 10. load -longitudinal steel strain curves for medium eccentricity ratio (e/h=0.65)

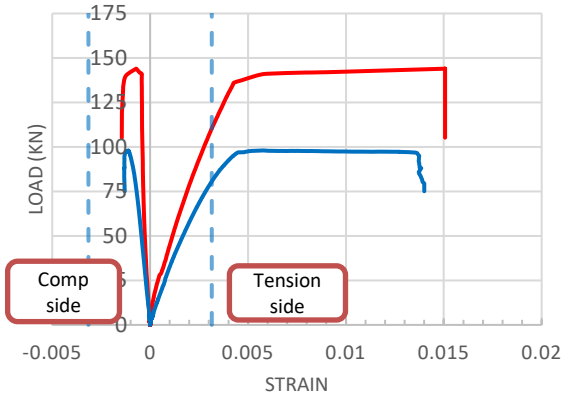

Figure 11. load -longitudinal steel strain curves for medium eccentricity ratio (e/h=0.90)

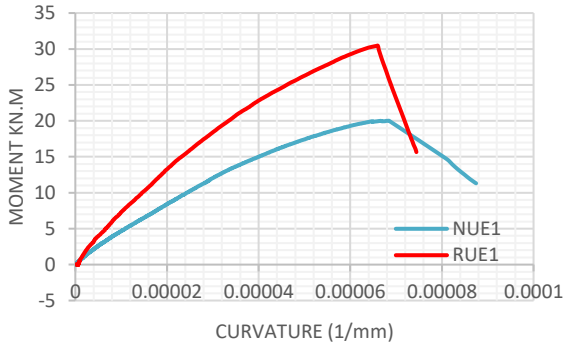

Figure 12. Moment-curvature curves for medium eccentricity ratio (e/h=0.25)

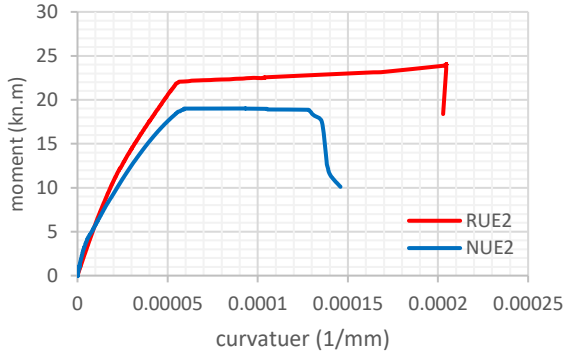

Figure 13. Moment-curvature curves for medium eccentricity ratio (e/h=0.65)

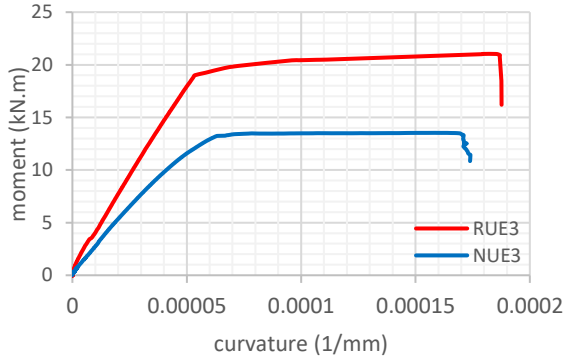

Figure 14. Moment-curvature curves for medium eccentricity ratio (e/h=0.9)

cross sections. Figures 12, 13 and 14 present the moment-curvature curves of the first and second groups of specimens and the third group of specimens respectively.

The bending moment (M) was given by the product of the applied load (P) and the true eccentricity. This true eccentricity was calculated by addition of the initial set eccentricity (e) to the critical net lateral deflection at mid-height (Δ) obtained in the prior stage. It is computed in Equation 1.

$$Mu= P(e+\Delta) \quad (1)$$

Curvature along the cross-sectional axis of the specimens was reported in a previous study. These curvatures were estimated using Equation 2,which assumes that plane sections remain plane after bending. Curvature (ϕ) was calculated as follows:

$$\Phi i = (\varepsilon_{sti}- \varepsilon_{sci})/d \quad (2)$$

Where (ε_{sti}) denotes the longitudinal strain in the tension reinforcement, (ε_{sci}) represents the longitudinal strain in the compression reinforcement, and (d) is the centre-to-centre distance of compression and tension reinforcements (114 mm for uniaxially loaded specimens).

A summary of the test results of the specimens subject to uniaxial eccentric loadings is also given in Table 5 and Figure 15. Data consist of the peak axial load (Pu), the lateral displacement at that peak load (Δu), and the ultimate bending moment, which is calculated as: Mu = Pu × (e + Δu). The table is also providing the percent increase or decrease in the bending moment (Mu).

The findings indicated that higher concrete strengths for the outer shell in hybrid sections resulted in enhanced flexural performance. In contrast, greater eccentricity ratios resulted in an appreciable decrease in the bending strength.

The substitution of the external shell veneer by reactive powder concrete (RPC) resulted in an evident increase of the flexural capacity. At low eccentricity ratio (ex/bx = 0.25), specimen RUE1 evidences an increase in resistance of 52.75% over the control specimen NUE1.

For the medium eccentricity (ex/bx = 0.65), RUE2 was 21.71% higher than NUE2. When the eccentricity ratio was large (ex/bx = 0.9), RUE3 was 55.99% higher than NUE3. These results are plotted in Figure 16. no analytical M–N interaction model was included due to

TABLE 5. Experimental findings (bending moment with curvature) for uniaxially loaded specimens

No.	Speci-men	Pu (kn)	Δ_u (mm)	Mu= Pu* (Δ_u+e) (kn.m)	Curvature (1/mm)	Increase in Mu (%)
1	NUE1	467.27	7.655	19.931	6.47E-05	0
2	RUE1	737.52	6.281	30.445	6.58E-05	52.751
3	NUE2	180.94	20.07	19.011	9.32E-05	0
4	RUE2	219.04	20.64	23.139	6.02E-05	21.713
5	NUE3	98.037	17.52	13.482	7.86E-05	0
6	RUE3	144.02	26.03	21.031	1.79E-04	55.993

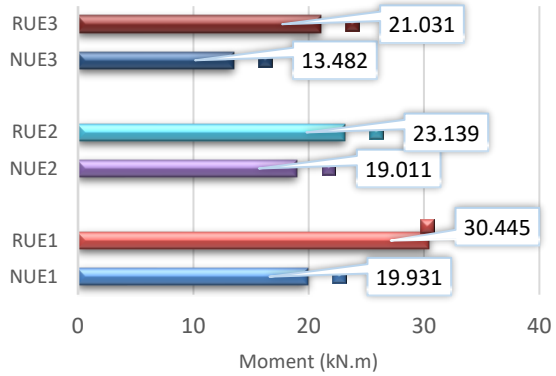

Figure 15. bending moments for column's specimens

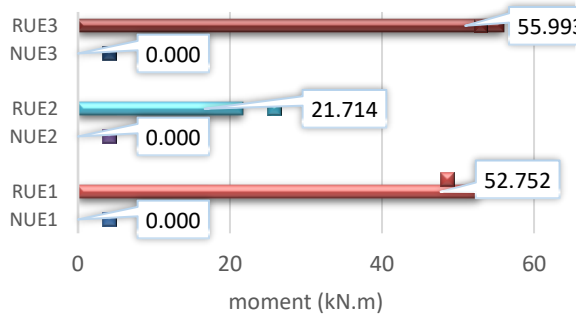

Figure 16. bending moments percentage according to reference specimens

the complex hybrid cross-section and the nonlinear behavior under high eccentricity.

8. 4. Evaluation of P–Δ Effectiveness To assess the impact of geometric nonlinearity in the tested slender columns, the second-order P–Δ moment was calculated as the product of peak axial load and the corresponding lateral displacement. This additional moment, arising from lateral instability, was compared with the primary eccentric moment to determine its relative influence.

As presented in Table 6, the P–Δ amplification ratio ranged between 12.21% and 18.49% across all specimens. These values confirm the noticeable effect of second-order behavior, especially in models subjected to higher eccentricities and larger deflections such as RUE2 and NUE2. In such cases, the additional moment significantly increased the internal moment demand, potentially accelerating failure due to lateral instability.

8. 5. FLEXURAL Energy Absorption The flexural energy absorption, estimated from the area under the moment–curvature (M–ϕ) curves, showed varied trends depending on the eccentricity ratio (e/h). For e/h = 0.25, the hybrid specimen (RUE1) absorbed more energy (2.423 kN) compared to the SC-NC specimen (NUE1: 1.725 kN). At e/h = 0.65, the SC-NC specimen (NUE2) exhibited greater absorption (3.850 kN) than its hybrid counterpart (RUE2: 2.389 kN). At the highest eccentricity (e/h = 0.90), the hybrid specimen (RUE3) again showed superior energy absorption (3.092 kN vs.

TABLE 6. P–Δ Moments and Amplification Ratios

Specimen	Pu (KN)	e (mm)	Δ (mm)	M_e	M_Δ	M_{total}	P-Δ ratio {%}
NUE1	467.27	35	7.66	16.35	3.58	19.93	17.95
RUE1	737.52	35	6.28	25.81	4.63	30.45	15.22
NUE2	180.94	91	20.07	16.47	3.63	20.10	18.07
RUE2	219.04	91	20.64	19.93	4.52	24.45	18.49
NUE3	98.037	126	17.52	12.35	1.72	14.07	12.21
RUE3	144.02	126	26.03	18.15	3.75	21.90	17.12

1.804 kN for NUE3). These findings highlight the influence of eccentricity on the flexural performance of hybrid sections, especially in enhancing post-cracking resistance. Figure17 show Energy of specimens.

8. 6. Mode of Failure Photographs of the tested columns under uniaxial eccentric loading are shown in Figure 18. A summary on observed failure modes and respective descriptions ara given in Table 7. In general, the tested sections presented flexural failure, that was strongly affected by the eccentricity also with respect to its value and position.

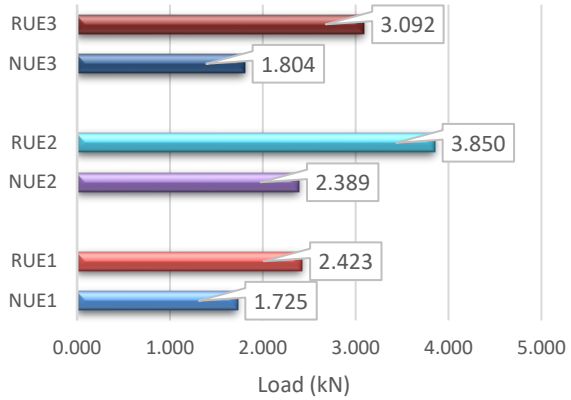

Figure 17. Energy for column's specimens

TABLE 7. Failure modes of specimens

Specimens	Failure modes	Description
NUE1	Compression failure	Suddenly concrete crushing in upper third of the column
RUE1	Compression failure	Suddenly concrete crushing in upper region of the column and a wide crack in upper third of the column.
NUE2	Flexural – compression failure	The appearance of cracks along the column in the tension zone, with gradual concrete crushing in the middle third in the compression zone.
RUE2	Flexural - ductile Buckling failure	The appearance of cracks along the column in the tension zone, with visible wide cracking in the mid-height of the column
NUE3	Flexural – compression failure	The appearance of cracks along the column in the tension zone, with gradual concrete crushing in the middle third in the compression zone.
RUE3	Flexural failure	Thin cracks are densely distributed along the length of the column.

Figure 18. Failure modes

9. CONCLUSION

This study experimentally investigated the structural behavior of slender hybrid reinforced concrete columns composed of a self-compacting core and outer shells made of either self-compacting normal concrete (SC-NC) or reactive powder concrete (SC-RPC), under uniaxial

and biaxial eccentric axial loads. Based on the obtained results and analysis, the following conclusions are drawn:

1. Substituting the SC-NC shell with SC-RPC significantly enhanced axial capacity. Compared to reference specimens, the axial load increased by 57.8%, 21.1%, and 46.9% for low (e/h = 0.25), moderate (0.65), and high (0.90) eccentricities, respectively, indicating the superior compressive performance of RPC in confined hybrid sections.
2. Moment capacity increased by 52.75%, 21.71%, and 55.99% at the respective eccentricities above. The improvement highlights RPC's significant contribution to flexural resistance, especially under high moment demands.
3. Second-order effects (P–Δ) became more pronounced with increasing eccentricity. The amplification ratio ranged from 12.21% to 18.49%, with hybrid columns (SC-RPC) exhibiting better control over lateral displacements, thus minimizing instability due to geometric nonlinearity.
4. The area under the moment–curvature (M–φ) curve showed enhanced energy dissipation in SC-RPC sections. Compared to SC-NC, the absorbed energy increased by 40.5% (RUE1), decreased in the mid-eccentricity case (RUE2), and peaked at +71.4% for RUE3, reflecting the efficient post-cracking performance of RPC in highly eccentric configurations.
5. With increasing eccentricity, failure shifted from compression-dominated to tension-controlled modes. RPC specimens exhibited higher curvature at peak loads, smoother softening behavior, and improved ductility. The failure pattern transformed from brittle crushing to more ductile flexural modes, ensuring more controlled and safer deformation.
6. Hybrid columns subjected to uniaxial eccentric loading maintained overall stability. Damage was more localized, and RPC-based sections exhibited superior lateral resistance compared to their SC-NC counterparts.
7. Load–deflection and M–φ curves confirmed that SC-RPC columns experienced reduced lateral deformation and more energy-dissipative behavior, especially under severe eccentricities.
8. The use of RPC in hybrid slender columns is promising for seismic-resistant and high-rise construction where ductility and energy absorption are vital. These findings underline the practical benefits of RPC beyond basic strength enhancement.

10. LIMITATIONS AND FUTURE WORK

This study was limited to an experimental investigation of the behavior of hybrid concrete columns under uniaxial eccentric axial loads. No numerical or analytical modelling was conducted as part of this study. While the results provide interesting data for structural performance, a predictive method is needed for more general use. Therefore, in the future, we are planning to construct finite element models and carry out analytical comparisons (such as M–N interaction analysis) to verify and generalize these observations to a broader parameter space.

11. REFERENCES

1. Committee A, editor Building code requirements for structural concrete (ACI 318-08) and commentary2008: American Concrete Institute.
2. Salman Al-Taai AA, Hassan SA, Hussein LF. Finite Element Analysis of Corner Strengthening of CFRP-Confined Concrete Column. 2018. https://doi.org/10.1088/1757-899X/454/1/012088
3. Al-Taai AAS. Finite Element Analysis of Concrete Filled Circular Steel Tube Short Columns Subjected to Axial Compression Load. Mathematical Modelling of Engineering Problems. 2025;12(5). https://doi.org/https://doi.org/10.18280/mmep.120523
4. Lai B, Liew JR, Venkateshwaran A, Li S, Xiong M. Assessment of high-strength concrete encased steel composite columns subject to axial compression. Journal of constructional steel research. 2020;164:105765. https://doi.org/https://doi.org/10.1016/j.jcsr.2019.105765
5. Lai B, Liew JR, Le Hoang A. Behavior of high strength concrete encased steel composite stub columns with C130 concrete and S690 steel. Engineering Structures. 2019;200:109743. https://doi.org/https://doi.org/10.1016/j.engstruct.2019.109743
6. Lai B, Liew JR, Wang T. Buckling behaviour of high strength concrete encased steel composite columns. Journal of Constructional Steel Research. 2019;154:27-42. https://doi.org/https://doi.org/10.1016/j.jcsr.2018.11.023
7. Begum M, Driver RG, Elwi AE. Behaviour of partially encased composite columns with high strength concrete. Engineering Structures. 2013;56:1718-27. https://doi.org/https://doi.org/10.1016/j.engstruct.2013.07.040
8. Mao W-J, Wang W-D, Zhou K, Du E-F. Experimental study on steel-reinforced concrete-filled steel tubular columns under the fire. Journal of Constructional Steel Research. 2021;185:106867. https://doi.org/10.1016/j.jcsr.2021.106867
9. Xie F, Chen J, Yu Q-Q, Dong X. Behavior of cross arms inserted in concrete-filled circular GFRP tubular columns. Materials. 2019;12(14):2280. https://doi.org/10.3390/ma12142280
10. Chen Z, Ning F, Song C, Liang Y. Study on axial compression bearing capacity of novel concrete-filled square steel tube columns. Journal of Building Engineering. 2022;51:104298. https://doi.org/10.1016/j.jobe.2022.104298
11. Liu J, Gao P, Lin X, Wang X, Zhou X, Chen YF. Experimental assessment on the size effects of circular concrete-filled steel tubular columns under axial compression. Engineering Structures. 2023;275:115247. https://doi.org/10.1016/j.engstruct.2022.115247
12. Hu H-S, Yang Z-J, Xu L, Zhang Y-X, Gao Y-C. Axial compressive behavior of square concrete-filled steel tube columns with high-strength steel fiber-reinforced concrete. Engineering Structures. 2023;285:116047. https://doi.org/10.1016/j.engstruct.2023.116047

13. Yuan F, Cao L, Li H. Axial compressive behaviour of high-strength steel spiral-confined square concrete-filled steel tubular columns. Journal of Constructional Steel Research. 2022;192:107245. https://doi.org/10.1016/j.jcsr.2022.107245
14. Patel VI, Liang QQ, Hadi MN. Numerical simulations of circular high strength concrete-filled aluminum tubular short columns incorporating new concrete confinement model. Thin-Walled Structures. 2020;147:106492. https://doi.org/10.1016/j.tws.2019.106492
15. Wang F-C, Zhao H-Y, Han L-H. Analytical behavior of concrete-filled aluminum tubular stub columns under axial compression. Thin-Walled Structures. 2019;140:21-30. https://doi.org/10.1016/j.tws.2019.03.019
16. Xu W, Zhang J, Liu F, Ma Z, Zhao G, Gu C, et al., editors. Axial compression behavior of assembled aluminum alloy-concrete-carbon steel double-skin tubular column. Structures; 2024: Elsevier.
17. Deng Z, Guo J, Yu J, Liu B. Axial compression performance of coral concrete-filled aluminium tube (CCFAT) square stub columns. Case Studies in Construction Materials. 2021;15:e00697. https://doi.org/10.1016/j.cscm.2021.e00697
18. Bu J, Liu Q, Yu Y, Qiu Q. Axial compression performance and bearing capacity calculation of round-ended concrete-filled aluminum tube column. Applied Sciences. 2023;13(13):7918. https://doi.org/10.3390/app13137918
19. Rong B, Zhai X, Li Z, Cheng H, Dong A, Zhang R. Study on axial compression behavior of 7A04-T6 concrete-filled aluminum tubular columns. Journal of Building Engineering. 2023;76:107118. https://doi.org/10.1016/j.jobe.2023.107118
20. Resheq A, editor Behaviour of hybrid concrete columns under axial compression loads. MATEC Web of Conferences; 2018: EDP Sciences.
21. Al-Zuhairi AH, Al-Ahmed AHA, Hanoon AN, Abdulhameed AA. Structural behavior of reinforced hybrid concrete columns under biaxial loading. Latin American Journal of Solids and Structures. 2021;18:e390. https://doi.org/10.1590/1679-78256640
22. Shariati M, Pourteymuri M, Naghipour M, Toghroli A, Afrazi M, Shariati M, et al. Evolution of confinement stress in axially loaded concrete-filled steel tube stub columns: study on enhancing urban building efficiency. Sustainability. 2024;16(17):7544. https://doi.org/10.3390/su16177544
23. Ali A, Mohammed Z. Strength evaluation of hybrid reinforced concrete columns under eccentric loads. Engineering and Technology Journal. 2018;36(4 Part A). https://doi.org/10.30684/etj.36.4a.12
24. ALI TKM. Experimental Behavior and Analysis of Hybrid Low-High Strength Reinforced Concrete Columns. Journal of Materials and Engineering Structures «JMES». 2020;7(2):203-14.
25. Ali AY, Mahdi WH. Experimental Investigation for Behavior of Reinforced Hybrid Concrete Corbel-Column System Subjected to Un-Symmetrical Vertical Loading. Journal of University of Babylon. 2017;25(2).
26. Hamid MM, Yassin LA, Mohammed AH, editors. Behavior of hybrid reinforced concrete columns. IOP Conference Series: Materials Science and Engineering; 2020: IOP Publishing.
27. Mohammed AH, Yassin LAG, Hamid MM. Experimental Investigation on the Ultimate Capacity of Rectangular Reinforced Hybrid Concrete Columns Under Axial Load. Geomate Journal. 2022;23(95):112-8. https://doi.org/10.21660/2022.95.3210
28. Hassan HF. Behavior of hybrid deep beams containing ultra high performance and conventional concretes. Engineering and Technology Journal. 2015;33(1):30-50. https://doi.org/10.30684/etj.33.1a.3
29. Danha L, Abdul-Hussien Z, Abduljabbar M, Yassin L, editors. Flexural behavior of hybrid ultra-high-performance concrete. IOP Conference Series: Materials Science and Engineering; 2020: IOP Publishing.
30. Hussein LF, Al-Taai AAS, Khudhur ID, editors. Sustainability achieved by using voided slab system. AIP Conference Proceedings; 2020: AIP Publishing LLC.
31. AYDIN E, OZTURK B, SAHIN E. Investigation of Behavior of Adjacent Planar Steel Frames Connected with Rigid Bars under Earthquake Effects.
32. Cetin H, Kebeli YE, Aydin E, Ozturk B, Ugu BA, editors. Experimental Evaluation of Tuned Mass Dampers for Seismic Vibration Control in Scaled Steel Structures. International Workshop on Energy-Based Seismic Engineering; 2025: Springer.
33. EFNARC S. guidelines for self-compacting concrete, English ed. European federation for specialist construction chemicals &concrete systems. 2005.
34. ASTM C. Standard specification for chemical admixtures for concrete. Annual book of ASTM standards. 2013.

Persian Abstract

چکیده

در این مقاله، بررسی جامعی از رفتار ستون‌های بتن آرمه هیبریدی باریک ارائه شده است که از پوسته‌هایی از بتن خودتراکم معمولی (SC-NC) و بتن پودری واکنشی-(SC RPC)تحت فشار خارج از مرکز با نسبت‌های مختلف برون‌مرکزی تشکیل شده‌اند. سه نسبت برون‌مرکزی (۰.۲۵، ۰.۶۵، و ۰.۹) برای انجام آزمایش‌ها روی شش نمونه استفاده شد که بر اساس نسبت برون‌مرکزی به سه گروه تقسیم شدند. هر گروه شامل یک نمونه مرجع با پوسته SC-NC معمولی و یک نمونه هیبریدی با پوسته RPC بود. نتایج نشان داد که استفاده از RPC باعث بهبود ظرفیت باربری محوری و ظرفیت خمشی می‌شود. مشخص شد که ظرفیت محوری به ترتیب به میزان ۵۷.۸٪، ۲۱.۱٪، و ۴۶.۹٪ برای برون‌مرکزی‌های کم، متوسط و زیاد افزایش یافت و ظرفیت خمشی نیز تا ۵۶٪ قابل افزایش است. نمونه‌های تقویت‌شده با RPC انرژی بیشتری را جذب کرده و جابجایی جانبی کمتری از خود نشان دادند. نتایج به‌طور مؤثر کارایی RPC را در بهبود عملکرد سازه‌ای و رفتار ستون‌های هیبریدی تحت بار محوری خارج از مرکز تأیید می‌کنند و می‌توانند دیدگاه‌های ارزشمندی برای کاربرد در سازه‌های مقاوم در برابر زلزله و بلندمرتبه فراهم کنند.